PROFESSOR SEYED JALAL HOSSEINIMEHR (Orcid ID : 0000-0001-8055-8036)

DR HAMID IRANNEJAD (Orcid ID : 0000-0001-7513-6162)

In vitro and in silico evaluation of P-glycoprotein inhibition through ^{99m}Tc-MIBI uptake

Seyed Sajad Hosseini Balef [1,2], Majid Piramoon[3,4], Seyed Jalal Hosseinimehr[3], Hamid Irannejad [2]

1 Student Research Committee, Mazandaran University of Medical Sciences, Sari, Iran

2 Department of Medicinal Chemistry, Faculty of Pharmacy, Mazandaran University of Medical Sciences, Sari, Iran

3 Department of Radiopharmacy, Faculty of Pharmacy, Mazandaran University of Medical Sciences, Sari, Iran

4 Faculty of Pharmacy, Lorestan University of Medical Sciences, Khorramabad, Iran

----

Corresponding authors: Dr. Hamid Irannejad (Computational part), Department of Medicinal Chemistry, Faculty of Pharmacy, Mazandaran University of Medical Sciences, Sari, Iran, E-mail: irannejadhamid@gmail.com. Dr. Seyed Jalal Hosseinimehr (Biologic part), Department of Radiopharmacy, Faculty of Pharmacy, Mazandaran University of Medical Sciences, Sari, Iran. E-mail: sjhosseinim@mazums.ac.ir. Phone: 0098-11-33543082, Fax: 0098-11-33543084

Abstract

P-glycoprotein (P-gp) is a multi-drug resistance (MDR) transporter with unknown structural details. This macromolecule is normally responsible for extruding xenobiotics from normal cells. Over-expression of P-gp in tumor cells is a major obstacle in cancer chemotherapy. In

this study, human 3D model of P-gp was built by homology modeling based on mouse P-gp crystallographic structure and stabilized through 1 ns molecular dynamic (MD) simulation. Stabilized human P-gp structure was used for flexible docking of 80 drugs into the putative active site of P-gp. Accordingly, digoxin, itraconazole, risperidone, ketoconazole, prazosin, verapamil, cyclosporine A, and ranitidine were selected for further *in vitro* assay. Subsequently, cell based P-gp inhibition assay was performed on Caco-2 cells while ^{99m}Tc-MIBI was used as a P-gp efflux substrate for calculating IC50 values. Results of the ^{99m}Tc-MIBI uptake in drugs-treated Caco-2 cells were in agreement with the previously reported activities. This study for the first time described the relation between molecular dynamics and flexible docking with cellular experiments using ^{99m}Tc-MIBI radiotracer for evaluation of potencies of P-gp inhibitors. Finally, results showed that our radiotracer-cell based assay is an accurate and fast screening tool for detecting P-gp inhibitors and non-inhibitors in drug development process.

Keywords: P-glycoprotein; ^{99m}Tc-MIBI; Caco-2; Homology modeling; Flexible docking

Running title: *In vitro* and in silico evaluation of P-gp inhibition

Introduction

One of the most important issues in cancer treatment is resistance to chemotherapeutic agents at later stages of disease. Several molecular mechanisms which are involved in drug resistance, have been identified and one is attributed to drug efflux pumps. Several membrane transporters exist which show resistance to conventional chemotherapy by conducting drug efflux such as P-glycoprotein (P-gp) (1). P-gp is a protein from the ATP Binding Cassette (ABC) superfamily. The Gene sequence of this protein has been cloned and determined in

human and consists of two important isoforms called MDR1 or ABCB1, which plays a role in drug efflux, and MDR2/MDR3 or ABCB4, which plays a role in transferring phosphatidylcholine to the bile. The drug transporter isoform (MDR1) has 78% sequence similarity with another isoform MDR3. P-gp is normally exists in blood brain barrier and blood testes barrier to limit the access of drugs to these vital tissues through effluxing drugs and xenobiotics out by ATP-dependent mechanism (2). MDR1 overexpression is associated with failure of chemotherapy in various cancer types like kidney, colon, and liver, as well as leukemia and lymphoma. MDR modulators are able to control the efflux of drugs as a result of P-gp modulation, which can address the resistance and improve the outcomes of cancer chemotherapy (3), (4). Owing to the poly-specificity in substrate binding and promiscuity in P-gp substrate structural features, developing a pharmacophore model for P-gp substrates or inhibitors has not been performed yet. In this sense, urge of designing and introducing potent and selective P-gp inhibitors is an aim in MDR. Therefore, developing a fast and accurate screening tool for determining substrate or inhibitor active site of P-gp and discriminating between substrates and non-substrates would be a valuable technique to overcome the MDR in cancer treatment.

^{99m}Tc-MIBI (^{99m}Tc-methoxyisobutylisonitrile) is widely used in nuclear medicine for cardiovascular imaging. This radiopharmaceutical agent is a substrate for P-gp, so that the accumulation of this radiotracer in tumor tissues can be cited as an indicator of the functionality of P-gp in tumors. Several studies have been shown that this radiolabeled compound can be used for detection of P-gp status in tumor cells. ^{99m}Tc-MIBI imaging has the advantage of a non-invasive approach to over-expression of P-gp gene in the *in vitro* environment (3), (5), (6).

The aim of this study is to model the 3D structure of the human P-glycoprotein and to predict a possible binding site of various ligands in the active site of this protein. In the following, the efficacy of P-gp efflux inhibition was investigated using ^{99m}Tc-MIBI uptakes in the drug-treated Caco-2 cells.

Materials and methods

In silico tools

A GNU/Linux personal Computer with 8 core CPU processors each of 3.0 GHz and 8 G RAM was employed for computational simulations. MODELLER v9.14 (7) for modeling the 3D structure of Human P-gp, Autodock Vina for flexible molecular Docking (8), Visual Molecular Dynamics (VMD) v1.9.2 (9), Chemaxon MarvinSketch v15.10.19.0, with academic license, for drawing 2D structure of drugs, Gromacs v5 for MD simulations and GraphPad Prism v5.03 for IC50 calculations were used.

In vitro materials

Dulbecco's Modified Eagle's medium (DMEM) and activated fetal bovine serum (FBS) were obtained from Gibco (USA); human epithelial colorectal adenocarcinoma (Caco-2) cell line has been purchased from Iranian Biological Resource Center (Iran); sodium hydroxide and dimethyl sulfoxide (DMSO) were obtained from Merck (Germany). Penicillin-Streptomycin and Trypsin-EDTA solution were obtained from Biowest (France). Cyclosporin A and digoxin were purchased from Zahravi (Iran); verapamil was obtained from Hexal (Germany); itraconazole and ranitidine were supplied from Tehran Darou (Iran); ketoconazole was from

Behvazan (Iran); risperidone was supplied from Abidi (Iran) and prazosin was kindly gifted by Temad (Iran). The drugs were dissolved in DMSO and diluted with DMEM medium.

3D structure of human P-gp

In order to find the best template sequence for human P-gp, sequences in BLAST (http://blast.ncbi.nlm.nih.gov) database were searched based on the MDR1. Among sequences retrieved, 3G61 (P-gp of *mus musculus*) was found as the best template with highest sequence similarity of 88% (10). 2D alignment and creating the model was performed and DOPE per-residue score diagram of the model and template were plotted and compared in MODELLER v9.14. Additionally, Ramachandran plot of the model was generated to evaluate the residues in favored region by RAMPAGE web interface (http://mordred.bioc.cam.ac.uk/~rapper/rampage.php). In the final step of P-gp model refinement, molecular dynamic simulation was performed with amber99sb force field to minimize the energy of predicted model, in GROMACS v5. An octahedral water box with 4.5 nm containing explicit atoms using TIP3P water model was generated. To neutralize the system, sodium (NA) and chlorine (CL) ions were added and replaced with water molecules. We performed an energy minimization by steepest decent for 50 ps with minimum 100 KJ/mol/nm cut-off followed by a 50 ps preprocessing. Then MD simulation performed for 1 ns. Finally, root mean square deviation (RMSD) of the stabilized protein during 1 ns versus the starting point structure was calculated. The details of MD parameters used are in Figure S5 in Supplementary material.

Ligand preparation

2D structures of ligand candidates as substrate, inhibitor or inducer of P-gp (80 drugs in Table S2 in Supplementary material) were selected from literature (11), sketched and protonated (pH=7.4) in MarvinSketch software. Energy minimization of molecules was performed using semiempirical PM3 method, in order to generate the most stable 3D conformer of each compounds.

Flexible Docking

3D structures of ligands and modeled human P-gp were imported in AutodockTools in order to do preprocessing steps, i.e. add hydrogens, calculating Gasteiger charges, torsions and then saving in PDBQT format. In the next step, TYR84, Ile27, TYR920, PHE39, PHE46, PHE70, PHE281, PHE303, PHE310, PHE695, PHE699, PHE924, PHE945, ILE703, LEU306, MET36, and GLN162 were assumed as flexible residues (12). Flexible docking was performed for 80 ligands using an in-house written bash script which employed Autodock Vina and Vina split, a subsidiary tool to split multiple-structure PDB-formatted files into single PDB files (13). Grid center was positioned on 77.088, 170.238, and 121.994 as x, y, and z cartesian coordinates, grid size was defined as 126×126×126 points and exhaustiveness was set to 8 for the docking procedure so as to include all 12 helices (14).

Cellular experiments

^{99m}Tc-MIBI is a substrate for the P-gp pump (15). ^{99m}Tc-MIBI was prepared according to manufacturer instruction (Pars Isotope, Iran) at day of experiment. ^{99m}TcO$_4$Na was freshly eluted from ^{99}Mo/^{99m}Tc generator (Pars Isotope, Iran) and added to MIBI kit and then the vial

content was shaken for a few seconds. Then the vial was placed in boiling water bath for 10 min and kept for 15 min at room temperature. The ^{99m}Tc-MIBI kit was diluted with normal saline for adjustment of radioactivity. Caco-2 cell line overexpresses P-gp and was selected in this study (16, 17). Caco-2 cells were cultivated at 37 °C in a 5% CO_2 incubator and were maintained in Dulbecco's DMEM-high glucose supplemented with 10% FBS. Cells were grown in T-flask, and after a period of time, cultures reached confluency. In this study, about forty million Caco-2 cells were grown and collected after two weeks' cell culture through passages in 175-cm^2 flasks. The Caco-2 cells were detached from flask with trypsin and then counted. For each drug treatment, cells were seeded at density of 2×10^5 cells per well in 24-well plates and cultured in DMEM medium with 10% (v/v) FBS and 1% penicillin–streptomycin in 5% CO_2 for 24 h. On the day of the experiment, cells were washed with cold serum-free DMEM. Then, drugs (cyclosporine A, digoxin, verapamil, itraconazole, ranitidine, ketoconazole, risperidone, prazosin) were added at different concentrations (0, 0.5, 1, 5, and 10 μM) to cells; and one row of plate was assigned to the negative control group (cell-free) to exhibit absorption of radiotracer to plastic of plates (n = 4). After incubation of cells with drugs for 30 min, 50 MBq of ^{99m}Tc-MIBI (100 μl) was added to each of wells and incubated for 30 min. All wells were washed twice using the DMEM medium free FBS and then cells were lysed with 2 ml of 0.1 M sodium hydroxide and collected in tubes. The radioactivity of each tube was counted as count per minute (CPM) with a NaI (Tl) gamma counter (Delshid, Iran).

The radioactivity (CPM) of each treated well was subtracted from CPM of negative control tube as absorption of radiotracer to plastic of plates to be background radioactivity. The radioactivity results were analyzed by graphical method, such that the graph of net CPM of each concentration against the log concentration of each drug was plotted and IC50 value was determined with GraphPad Prism software. To normalize the series of curves, the data were

then converted to percentage inhibition curve. IC50 is concentration of a drug to show 50% CPM of radiotracer in Caco-2 cells in which the drug has been accumulated.

Statistical analysis

For statistical analysis, GraphPad Prism 6 software (Graph Pad, La Jolla, CA, USA) was used for IC50 calculation. Comparing of groups was done by unpaired t-test. For all tests, *P* values less than 0.05 were considered as significant.

Results

3D structure of human P-gp

The result of finding the best template structure for human MDR1 for homology modeling is presented in Table S1 in Supplementary material as the top 10 template structures with their percent of homology. The best template with highest percent of homology was found for 3G61 with 88% sequence similarity and its single alignment is illustrated in Figure S1 in Supplementary material. The normalized Discrete Optimized Potential Energy (DOPE) per-residue score of the final model and 3G61 PDB file were plotted and is presented in Figure S2. As seen, the green line (MDR1) is under the zero value threshold for all residues and confirms the low energy value of each residue in entire MDR1 protein structure.

Moreover, Ramachandran and RMSD plot of the modeled human P-gp, after running 1 ns dynamic simulation with amber99sb force field, are presented in Figures S3 and S4 in Supplementary material. As seen in the RMSD plot, protein structure has reached a plateau

after 800 ps of simulation and does not change significantly during the last 200 ps of simulation.

According to the Ramachandran plot, the number of residues in favored region is 92.3%, 6.8% in allowed region and 0.9% in disallowed region, indicating that our homology modeled P-gp is suitable for further structural analysis and drug binding studies at the active site. The final modeled P-gp structure is available as a PDB file in Supplementary material.

In order to define a possible P-gp active site and to choose a few compounds with various activities as substrate, inhibitor or inducer of P-gp for in vitro ^{99m}Tc-MIBI uptake in Caco-2 cells, flexible docking was performed for 80 drugs listed in Table S2 in Supplementary material. These 80 drugs were previously reported to be as substrate, inhibitor or inducer (interaction type in Table S2) of P-glycoprotein (11). In this study, key residues in the hydrophobic channel of P-gp such as TYR84, Ile27, TYR920, PHE39, PHE46, PHE70, PHE281, PHE303, PHE310, PHE695, PHE699, PHE924, PHE945, ILE703, LEU306, MET36, and GLN162 were considered to be flexible during docking performance. The scores of docking calculations via Autodock vina in kcal/mol for 80 drugs along with their binding cluster and interaction types are presented in Table S2 and their predicted binding sites within the P-gp structure are illustrated in Figure 1 (PDB file of the complex P-gp and docked drugs are available in Supplementary material). As seen in Figure 1, drugs are totally divided into 7 binding clusters as indicated by different colors. The most populated binding space (cluster A in red, 37 drugs) is predicted to be in the bottom of funnel shaped hydrophobic channel of P-glycoprotein as indicated by red color. Bound conformations with green and yellow colors were also estimated to be at second and third order of magnitude, 15 and 14 drugs respectively, and their binding space is near to the nucleotide binding domain. Clusters D and E with total 6 drugs were also found to bind near to the space occupied by cluster A. The least populated clusters F and G, each one with 2 drugs were found to be positioned next to

the nucleotide binding domain. The remaining drugs, mannitol, captopril, fluvoxamine and ranitidine were individually bound to the different parts of P-gp (Figure 1). Thereafter, eight drugs were selected from various clusters for further in vitro assessment of ^{99m}Tc-MIBI uptake in Caco-2 cells. The selected drugs are as follows: digoxin and risperidone in cluster A, ketoconazole and verapamil in cluster B, itraconazole and prazosin in cluster C, cyclosporine A in cluster F, and ranitidine as bolded in Table S2.

Figure 1.

Cellular experiment

The P-gp inhibition effects of selected drugs were examined on cultured Caco-2 cells with ^{99m}Tc-MIBI as a substrate by treating cells to different concentrations of drugs. It was clear that Caco-2 cells are able to uptake and accumulate ^{99m}Tc-MIBI radiotracer. The concentration-dependent radiotracer uptake was observed in the cells treated with P-pg inhibitors. The IC50 values of selected drugs are shown in Table 1. Itraconazole exhibited lowest IC50 (0.499 μM) with highest potency of P-gp inhibition while risperidone had highest IC50 (>100 μM) and lowest efficacy on P-gp inhibition in these tested drugs.

Table 1.

Discussion

This study for the first time described the relation between molecular dynamic and flexible docking with cellular experiments using ^{99m}Tc-MIBI radiotracer for evaluation of potencies of P-gp inhibitors. The IC50 values of P-gp inhibitors were compared with other studies that were determined by different methods. Basically, P-gp is composed of two homologous parts,

each consists of six transmembrane helices and a nucleotide binding domain (NBD) which are connected by flexible linker residues. Totally, twelve transmembrane helices constitute a hydrophobic channel predominantly coated by non-polar amino acids trough which, substrates are transferred out of the cell (18). It has been cleared that structurally diverse set of compounds can interact with P-gp and transported through cell membrane, indicating multiple binding sites with different chemical natures within its structure. Since no well-defined crystallographic 3D structure of human P-gp has been revealed yet, one of the methods to achieve and elucidate the 3D structure of P-gp is homology modeling. In our study, human P-gp structure was created by homology modeling of 3G61 (P-gp of *mus musculus*) as template with sequence similarity of 88% to human P-gp sequence. Analysis of the modeled structure by DOPE per-residue score diagram and Ramachandran plot indicated its reliable structure for further computational approaches. Since considering key residues in the P-gp binding cavity as flexible is crucial for obtaining reasonable results (19), flexible molecular docking was performed on the human modeled P-gp structure for 80 drugs which were previously reported to be substrate, inhibitor or inducer of P-gp. Accordingly, their docking scores in kcal/mol along with their binding cluster type are listed in Table S2 and illustrated in Figure 1. Due to the complexity and promiscuity of substrate binding, docking energy scores are not useful and determinant for distinguishing substrates, inhibitors and inducers (20). But the strength point obtained by these calculations is the predicted binding sites within the P-gp structure. As depicted in Figure 1, docked molecules are mainly bound in 7 different locations shown by colors. Most of the drugs (cluster A in red, 37 molecules) have been positioned in the apical part of the funnel-shaped hydrophobic channel. This space has been mentioned as a main part for substrate binding when P-gp is in its inward-facing conformation. After ATP binding to nucleotide binding domain (NBD), significant structural changes tend to outward-facing conformation and release of drugs out of cell (21). As shown

in Table S2, digoxin and risperidone have the lowest binding energies (-12.40 and -10.00 kcal/mol) in cluster A, and subsequently were selected for further *in vitro* assessments. The results of calculated IC50 values for *in vitro* assessment of ^{99m}Tc-MIBI uptake in Caco-2 cells showed that digoxin and risperidone have IC50 values of 7.055 and >100 μM respectively. These data obviously show that digoxin is a potent inhibitor but risperidone does not have any inhibitory effect on P-gp and probably would be only a substrate. This finding is in accordance with Barecki-Roach and colleagues who claimed that compounds which are substrate for P-gp may not be able to inhibit the function of this glycoprotein (22).

Essential binding interactions formed by digoxin in the hydrophobic channel and its binding location between transmembrane helices are illustrated in Figure 2. As shown, most of the interactions are hydrophobic formed by non-polar amino acids such as valine, alanine, isoleucine and phenylalanine. Due to the presence of several hydroxyl groups or oxygen atoms in the structure of digoxin, hydrogen bonding by serine and threonine residues contribute to the strong binding of digoxin.

Figure 2.

In cluster B shown by green, verapamil and ketoconazole were selected for *in vitro* assessment of ^{99m}Tc-MIBI uptake. IC50 values calculated for these two drugs were 3.353 and 2.457 μM respectively for verapamil and ketoconazole and show that these two drugs are potent inhibitors of P-gp. In a study reported by Achira and colleagues regarding the interaction of P-gp and cytochrome P450 3A4 specific inhibitors, the IC50 of ketoconazole was calculated to be 3 μM in which vinblastine was used as P-gp substrate (23). In a different study done by Kishimoto et al., calculated IC50 of ketoconazole was reported to be 3.4 μM for P-gp inhibition while using dabigatran etexilate as substrate (24).

Our obtained data for verapamil is also in accordance with studies of Perloff and colleagues who reported IC50 values of 6.5 and 2.6 μM for verapamil as an inhibitor of fexofenadine and rhodamine 123 transport, respectively (25). It is clear that the IC50 values of ketoconazole and verapamil as P-gp inhibitors which were determined by ^{99m}Tc-MIBI is similar to other reported methods.

2D interactions of ketoconazole is presented in Figure S6 in Supplementary material, and shows formation of various types of interactions such as pi-pi, pi-alkyl, van der waals and pi-cation/anion.

Subsequently, itraconazole and prazosin were drug candidates from cluster C (yellow color in Figure 1) for *in vitro* evaluation of ^{99m}Tc-MIBI uptake in Caco-2 cells. Results indicated that itraconazole is the most potent inhibitor among compounds tested in our study with IC50 value of 0.499 μM. Moreover, IC50 value for prazosin was found to be 4.055 μM which shows its P-gp inhibition potential. The interacting amino acids with the type of interactions for prazosin are illustrated in Figure S7. Accordingly, in a study by Volpe and colleagues in 2013, to determine various parameters affecting IC50 for inhibitors of P-gp, IC50 value for itraconazole was shown to be 0.376 μM while digoxin was used as substrate (26). In a study conducted by Kishimoto et al., taking dabigatran etexilate into account as substrate, IC50 value of itraconazole was equal to 0.46 μM (24). It is clear that the IC50 value of itraconazole as a potent P-gp inhibitor which was determined with ^{99m}Tc-MIBI is close to the other reported methods.

The two cyclic peptides, cyclosporine A and valspodar in binding cluster F, were predicted to bind in a much larger space provided by helices in the basal segment of P-gp. This finding is consistent with the results reported for cyclic peptides for their similar binding site (19). This space is made by helices getting away from each other and to provide a spacious binding site

suitable for bulky substrates. Calculated IC50 value of cyclosporine A was found to be 3.35 μM and clearly shows its inhibition potential and ability to block ^{99m}Tc-MIBI transport across Caco-2 cell membrane.

Ranitidine as one of our tested compounds for in vitro evaluation of ^{99m}Tc-MIBI uptake in Caco-2 cells, showed IC50 value of 1.953 μM. This value explicitly indicates that ranitidine has molecular interactions at P-gp active site and is able to easily inhibit the outward transport of ^{99m}Tc-MIBI. Interestingly, ranitidine bound conformation predicted by docking calculations was shown to be located individually within P-gp. Its individual and unique location is obviously attributed to its hydrophilic nature as indicated by its logP of 0.99. The binding cavity of ranitidine is mostly surrounded by polar and hydrophilic amino acids such as Arg431, Lys347, Glu880, Glu126, Arg124, His120, Lys339 and Asp337 as shown in Figure S8.

In a study by Jara et al., a molecular docking tool was used to find out the active site of P-glycoprotein substrates and inhibitors. In the same study, several chemical compounds, including Rhodamine-123 and Propafenone, were docked in hydrophobic P-gp cavity to determine the proper active site in the protein. The results of the calculated Gibbs free energies showed that P1 site, consisting of 4,5,6 and 12 helices, was the best place for binding of substrates and inhibitors and the most important amino acids for binding were introduced as PHE299, PHE339, VAL334, LEU335 and SER218 (27). Similarly, the same space was predicted to be the main binding site for most of the compounds in our study. This space within P-gp has a hydrophobic chemical environment and is a favorite location for binding most of the drugs. In addition, in the study of Jara et al., It was suggested that hydrophobicity and molecular flexibility can be considered as two essential properties of P-gp inhibitory feature. Similarly, molecular volume, hydrophobicity and aromaticity have been proposed by QSAR and molecular docking to be essential features of P-gp inhibition (28).

Conclusion

As noted, our flexible docking procedure could substantially elucidate the main binding space of P-gp substrate or inhibitors which is located at the tip of the P-gp funnel shaped (binding cluster A). This binding location has been introduced in many previous studies as a principal binding site for P-gp substrates. Also our study showed that lipophilicity and molecular size are fundamental factors affecting and determining the location of P-gp binding site as seen in ranitidine and cyclosporine A. Furthermore, the results obtained by our method using cellular ^{99m}Tc-MIBI radiotracer uptake for evaluation of P-gp inhibition potency were consistent with other experimental methods which were recently reported. Therefore, for the first time, our study showed that cellular ^{99m}Tc-MIBI radiotracer uptake is a reasonable method for evaluation of P-gp inhibitor potencies.

Conflict of interest

Authors declare no conflict of interest.

Legends

Table 1. Calculated IC50 of drugs for in vitro assessment of ^{99m}Tc-MIBI uptake in Caco-2 cells.

Figure 1. Clustering of bound conformations of 80 drugs within modeled P-gp structure and are shown by different colors. Cluster A is shown in red, B in green, C in yellow, D in blue, E in purple, F in aqua and G in brown.

Figure 2. (A) 2D map of interacting amino acids with digoxin in binding cluster A, (B) Binding conformation of digoxin in the hydrophobic channel of P-gp constituted by transmembrane helices.

Table S1. The top 10 template structures with their PDB code and percent of homology to human MDR1.

Figure S1. 2D alignment of MDR1 and 3G61.

Figure S2. DOPE per-residue score diagram of MDR1 and 3G61.

Figure S3. Ramachandran plot of modeled MDR1.

Figure S4. RMSD plot of model in 1 ns MD.

Figure S5. MD parameters used in this study.

Table S2. Docking scores and binding cluster of 80 drugs for the putative active site of P-gp in kcal/mol. The bolded drugs were selected for in vitro assessment of ^{99m}Tc-MIBI uptake in Caco-2 cells. Clusters are indicated as A, B, C, D, E, F and G. Substrate, inhibitor or inducer characteristic of each drug is indicated in a separate column by Subs (substrate), Inh (inhibitor) and inducer (Ind). Bolded drugs were selected for in vitro cell-based inhibition assay.

Figure S6. 2D map of interacting amino acids along with their interaction types for ketoconazole in binding cluster B.

Figure S7. Schematic representation of prazosin in binding cluster C and the interacting amino acids.

Figure S8. 2D map of ranitidine in its bound conformation surrounded by mostly hydrophilic amino acids.

References

1.   Holohan C, Van Schaeybroeck S, Longley DB, Johnston PG (2013) Cancer drug resistance: an evolving paradigm. *Nat Rev Cancer;***13**: 714-26.

2.   Silva R, Vilas-Boas V, Carmo H, Dinis-Oliveira RJ, Carvalho F, de Lourdes Bastos M, et al. (2015) Modulation of P-glycoprotein efflux pump: induction and activation as a therapeutic strategy. *Pharmacol Ther;***149**: 1-123.

3.   Chai X, Liu Q, Shao W, Zhang F, Wang X, Wang H (2012) Bromocriptine enhances the uptake of (99m)Tc-MIBI in patients with hepatocellular carcinoma. *J Biomed Res;***26**: 165-9.

4.   Yamaguchi H, Kidachi Y, Kamiie K, Noshita T, Umetsu H (2012) Homology modeling and structural analysis of human P-glycoprotein. *Bioinformation;***8**: 1066-74.

5.   Krasznai ZT, Toth A, Mikecz P, Fodor Z, Szabo G, Galuska L, et al. (2010) Pgp inhibition by UIC2 antibody can be followed in vitro by using tumor-diagnostic radiotracers, 99mTc-MIBI and 18FDG. *Eur J Pharm Sci;***41**: 665-9.

6.   Swift B, Yue W, Brouwer KL (2010) Evaluation of (99m)technetium-mebrofenin and (99m)technetium-sestamibi as specific probes for hepatic transport protein function in rat and human hepatocytes. *Pharm Res;***27**: 1987-98.

7.   Webb B, Sali A (2014) Comparative Protein Structure Modeling Using MODELLER. *Curr Protoc Bioinformatics;***47**: 5 6 1-32.

8.   Sanner MF (1999) Python: a programming language for software integration and development. *J Mol Graph Model;***17**: 57-61.

9.   Humphrey W, Dalke A, Schulten K (1996) VMD: visual molecular dynamics. *J Mol Graph;***14**: 33-8, 27-8.

10.   Altschul SF, Madden TL, Schaffer AA, Zhang J, Zhang Z, Miller W, et al. (1997) Gapped BLAST and PSI-BLAST: a new generation of protein database search programs. *Nucleic Acids Res;***25**: 3389-402.

11.   Wang YH, Li Y, Yang SL, Yang L (2005) Classification of substrates and inhibitors of P-glycoprotein using unsupervised machine learning approach. *J Chem Inf Model;***45**: 750-7.

12.   Martinez L, Arnaud O, Henin E, Tao H, Chaptal V, Doshi R, et al. (2014) Understanding polyspecificity within the substrate-binding cavity of the human multidrug resistance P-glycoprotein. *FEBS J;***281**: 673-82.

13.   Hosseini Balef SS, Chippindale AM, Irannejad H (2018) A crystallographic and theoretical study of an (E)-2-Hydroxyiminoethanone derivative: prediction of cyclooxygenase inhibition selectivity of stilbenoids by MM-PBSA and the role of atomic charge. *J Biomol Struct Dyn;*1-12. https://doi.org/10.1080/07391102.2018.1462256

14.   McCormick JW, Vogel PD, Wise JG (2015) Multiple Drug Transport Pathways through Human P-Glycoprotein. *Biochemistry;***54**: 4374-90.

15.   Hendrikse NH, Franssen EJ, van der Graaf WT, Meijer C, Piers DA, Vaalburg W, et al. (1998) 99mTc-sestamibi is a substrate for P-glycoprotein and the multidrug resistance-associated protein. *Br J Cancer;***77**: 353-8.

16.   Sun H, Chow EC, Liu S, Du Y, Pang KS (2008) The Caco-2 cell monolayer: usefulness and limitations. *Expert Opin Drug Metab Toxicol;***4**: 395-411.

17.   Anderle P, Niederer E, Rubas W, Hilgendorf C, Spahn-Langguth H, Wunderli-Allenspach H, et al. (1998) P-Glycoprotein (P-gp) mediated efflux in Caco-2 cell monolayers: the influence of culturing conditions and drug exposure on P-gp expression levels. *J Pharm Sci;***87**: 757-62.

18.   Chen CJ, Chin JE, Ueda K, Clark DP, Pastan I, Gottesman MM, et al. (1986) Internal duplication and homology with bacterial transport proteins in the mdr1 (P-glycoprotein) gene from multidrug-resistant human cells. *Cell;***47**: 381-9.

19.   Dolghih E, Bryant C, Renslo AR, Jacobson MP (2011) Predicting binding to p-glycoprotein by flexible receptor docking. *PLoS Comput Biol;***7**: e1002083.

20.   Demel MA, Kramer O, Ettmayer P, Haaksma EE, Ecker GF (2009) Predicting ligand interactions with ABC transporters in ADME. *Chem Biodivers;***6**: 1960-9.

21.   Ward A, Reyes CL, Yu J, Roth CB, Chang G (2007) Flexibility in the ABC transporter MsbA: Alternating access with a twist. *Proc Natl Acad Sci U S A;***104**: 19005-10.

22.   Barecki-Roach M, Wang EJ, Johnson WW (2003) Many P-glycoprotein substrates do not inhibit the transport process across cell membranes. *Xenobiotica;***33**: 131-40.

23.   Achira M, Suzuki H, Ito K, Sugiyama Y (1999) Comparative studies to determine the selective inhibitors for P-glycoprotein and cytochrome P450 3A4. *Aaps Pharmsci;***1**:

24.   Kishimoto W, Ishiguro N, Ludwig-Schwellinger E, Ebner T, Schaefer O (2014) In Vitro Predictability of Drug-Drug Interaction Likelihood of P-Glycoprotein-Mediated Efflux of Dabigatran Etexilate Based on [I](2)/IC50 Threshold. *Drug Metab Dispos;***42**: 257-63.

25.   Perloff MD, von Moltke LL, Greenblatt DJ (2002) Fexofenadine transport in Caco-2 cells: Inhibition with verapamil and ritonavir. *J Clin Pharmacol;***42**: 1269-74.

26.   Volpe DA, Hamed SS, Zhang LK (2014) Use of Different Parameters and Equations for Calculation of IC50 Values in Efflux Assays: Potential Sources of Variability in IC50 Determination. *Aaps J;***16**: 172-80.

27.   Jara GE, Vera DM, Pierini AB (2013) Binding of modulators to mouse and human multidrug resistance P-glycoprotein. A computational study. *J Mol Graph Model;***46**: 10-21.

28.   Tan W, Mei H, Chao L, Liu T, Pan X, Shu M, et al. (2013) Combined QSAR and molecule docking studies on predicting P-glycoprotein inhibitors. *J Comput Aided Mol Des;***27**: 1067-73.

Table 1. Calculated IC50 of drugs for in vitro assessment of ^{99m}Tc-MIBI uptake in Caco-2 cells.

Drugs	Calc. logP	IC50 (µM)
Cyclosporine A	3.64	3.35
Risperidone	2.63	>100
Ranitidine	0.99	1.953
Ketoconazole	4.19	2.457
Itraconazole	7.31	0.499
Digoxin	2.73	7.055
Prazosin	1.65	4.055
Verapamil	5.04	3.353

logP calculated by ChemAxon.

Cytosol

Extracellular space
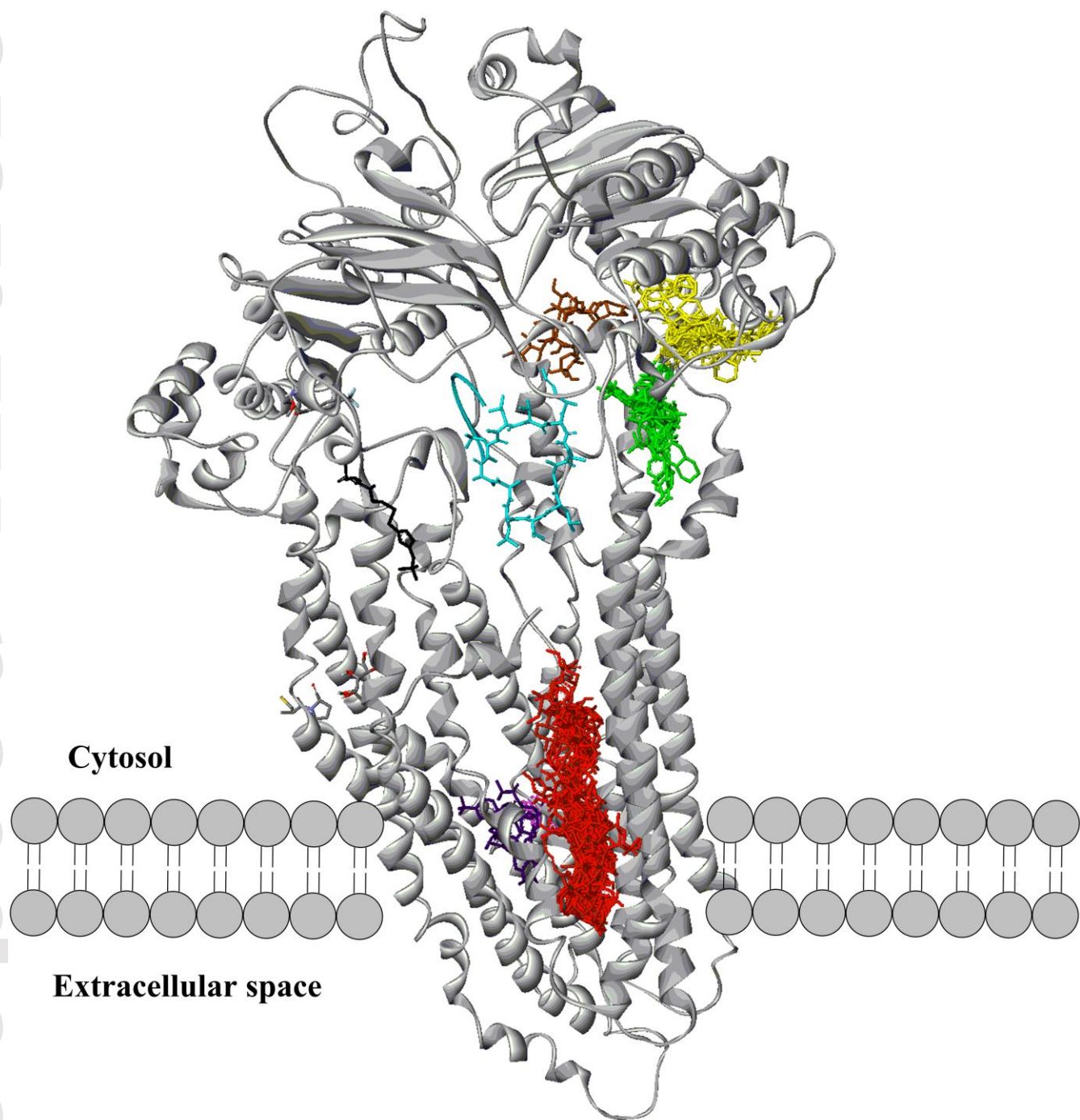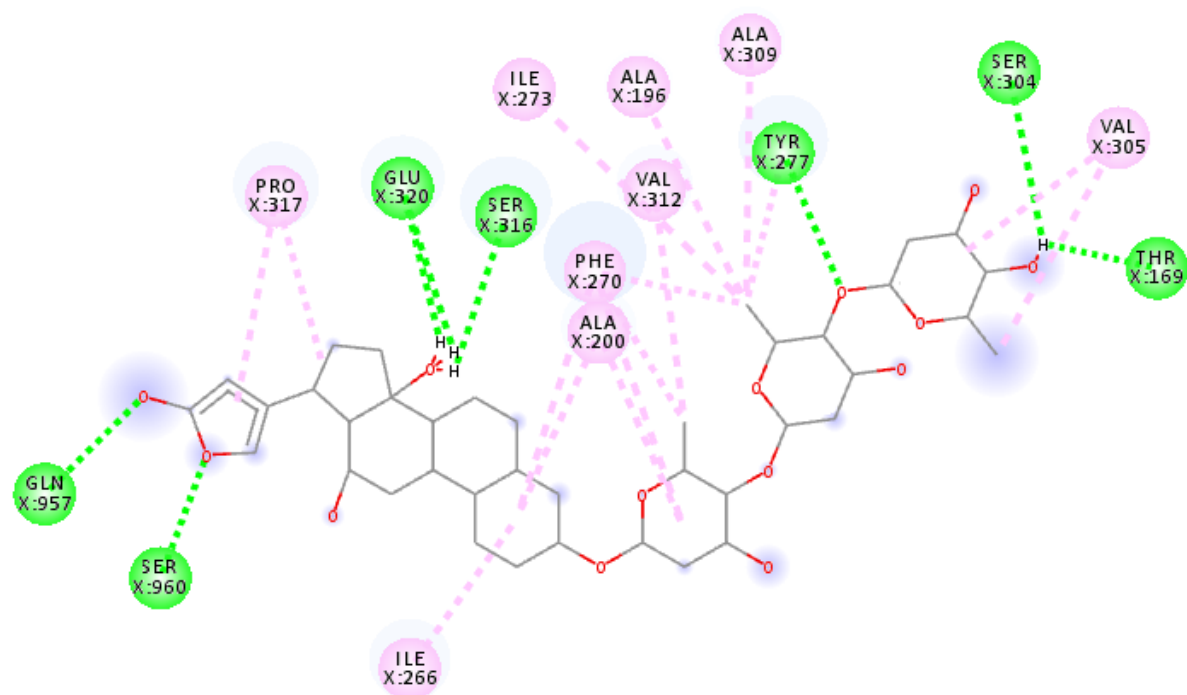
Interactions

- ■ (green) Conventional Hydrogen Bond
- ■ (pink) Alkyl
- ■ (pink) Pi-Alkyl